A Bis-Alkylating Triplex Forming Oligonucleotide Inhibits Intracellular Reporter Gene Expression and Prevents Triplex Unwinding Due to Helicase Activity†

Amy J. Ziemba,‡ Michael W. Reed,§ Kevin D. Raney,⊥ Alicia B. Byrd,⊥ and Scot W. Ebbinghaus*,‡

Arizona Cancer Center, University of Arizona, Tucson, Arizona, Epoch Biosciences, Bothell, Washington, and University of Arkansas for Medical Sciences, Little Rock, Arkansas

Received December 5, 2002; Revised Manuscript Received March 10, 2003

ABSTRACT: Triplex forming oligonucleotides (TFOs) have the ability to site specifically modulate gene expression through the formation of triple helix DNA. The HER-2/neu promoter contains a strategically located triplex target sequence, and has been successfully targeted in vitro, with little success in vivo. A TFO was conjugated at both its 5′ and 3′ ends to an alkylating agent (phenylacetate mustard) in an attempt to stabilize the triple helix intracellularly. In vitro assays demonstrated that the bis-conjugate bound the duplex and alkylated the target guanine residues with high efficiency. The bis-conjugate suppressed promoter activity by 60−70% in cancer cells using a plasmid with a preformed triple helix, and the suppression was minimal when the nitrogen mustard was conjugated at only one end. Helicase assays demonstrated that helicase activity can unwind the TFO at the unalkylated end of the triple helix, which may leave the unwound oligonucleotide susceptible to nuclease degradation or ineffective at inhibiting transcription initiation. Our findings indicate that dual alkylation of the target sequence is required to suppress the intracellular activity of a reporter plasmid with a preformed triple helix, likely due to greater stability of the triple helix within cells and inhibition of helicase activity.

The use of triplex forming oligonucleotides (TFOs)[1] to regulate endogenous gene expression has been an important but elusive goal for over a decade. This strategy utilizes TFOs designed to recognize highly specific duplex DNA tracts within a large heterogeneous DNA population. TFOs bind site-specifically to purine/pyrimidine-rich DNA tracts through Hoogsteen hydrogen bonds to form triple helix DNA (*1*, *2*). The formation of an intermolecular triple helix can hinder gene expression at the level of transcription (*3*) or may be used to introduce site-specific mutations (*4*). The use of TFOs to regulate gene expression at the transcriptional level has the potential advantage of targeting a limited number of DNA molecules and may be more efficient than strategies that target an amplified mRNA or protein. Triplex target sequences have already been identified in a number of important genes, such as c-myc, EGF-R, HIV-1, and HER-2/neu (*5*−*9*). If successful, TFOs may represent therapeutic agents to treat cancers or viral diseases that overexpress triplex target genes.

HER-2/neu is overexpressed in numerous types of human cancer, such as carcinomas of the breast and lung, and can be a predictor of shortened survival time (*10*−*12*). Current strategies that target the HER-2/neu gene product suggest that suppression of HER-2/neu expression may be of clinical benefit in the treatment of cancer (*13*, *14*). The HER-2/neu gene contains two triplex target sites that have both been successfully targeted in vitro. One site is located within the coding sequence, and triplex formation at this site has been shown to inhibit RNA polymerase elongation (*8*). The other site is located within the promoter region from bases −218 to −245 relative to the translation start site, and its location between two important promoter regulatory regions imparts the potential for triplex formation to significantly modify gene expression through inhibition of transcription initiation (see Figure 1). The TFO may prevent binding of critical positive trans-acting factors that are important regulators of promoter activity. Previous studies have demonstrated triplex formation at the HER-2/neu promoter inhibits protein binding and transcription initiation in vitro, and can specifically prevent binding of the transcription factor PU.1, an *ets* family member, to its recognition sequence adjacent to the triplex target sequence (*9*, *15*).

While there have been numerous successes using triplex technology to regulate gene expression in vitro, direct evidence of triple helix formation at the desired endogenous gene target and subsequent regulation of gene expression have not yet been achieved. However, a number of recent reports strongly imply triplex formation at the intended target in living cells. For example, TFOs have been successfully utilized to introduce site-specific DNA mutations in yeast, mammalian cell culture, and the mouse genome (*4*, *16*, *17*). Moreover, multiple reports indicate that plasmid DNA with a preformed triple helix demonstrated triplex-specific inhibi-

† This research was funded by the National Institutes for Health Grant CA85306 and the Flinn Foundation Grant 1316.

* To whom correspondence should be addressed. Scot W. Ebbinghaus, MD, Arizona Cancer Center, 1515 N Campbell Ave., Tucson, AZ 85724. Phone: (520) 626−3424. Fax: (520) 626−3754. E-mail: sebbinghaus@azcc.arizona.edu.

‡ University of Arizona.

§ Epoch Biosciences.

⊥ University of Arkansas for Medical Sciences.

[1] Abbreviations: TFO, triplex forming oligonucleotide; PAM, phenylacetate mustard; CHL, chlorambucil; NER, nucleotide excision repair; BER, base excision repair; PPG, pyrazolopyrimidine guanine; ODN, oligonucleotide; WCE, whole cell extracts.

10.1021/bi0273112 CCC: $25.00
Published on Web 04/09/2003

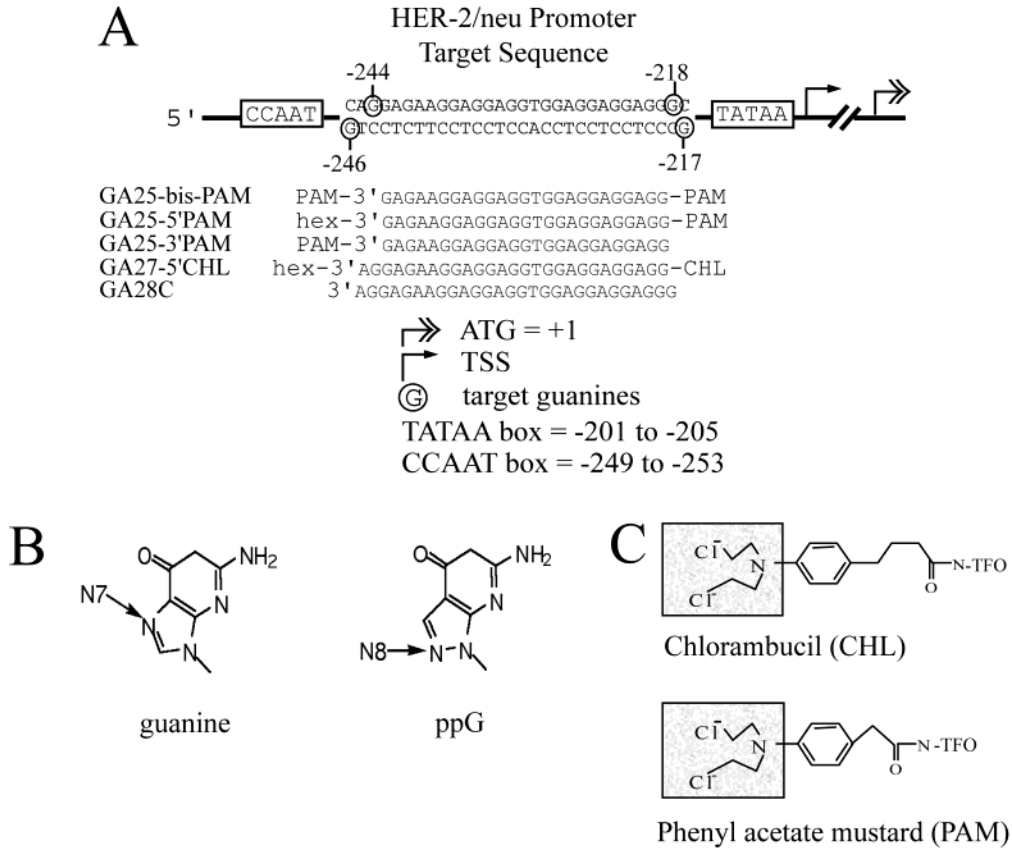

FIGURE 1: Triplex target and TFO components. **(**A) Schematic representation of the HER-2/neu promoter triplex target sequence. The target sequence is a 28-bp purine/pyrimidine-rich tract located between the CCAAT and TATAA boxes. The numbering is based upon the translation start site as +1, with the primary transcription start site (TSS) at −120. The TFO binding sequences and orientations are indicated beneath the target sequence, and the guanine residues targeted for nitrogen mustard alkylation are circled. (B) Comparison of guanine and a guanine analogue known as pyrazolopyrimidine guanine (PPG). (C) Chemical structures of the nitrogen mustards chlorambucil (CHL) and phenylacetate mustard (PAM). The chloroethylamine groups responsible for N7 alkylation are highlighted.

tion of gene expression in transfected cancer cells (*18*−*20*). One study demonstrated great potential for endogenous gene targeting via TFOs by physically demonstrating that an integrated HIV-1 proviral genome was accessible to triplex formation by a TFO-psoralen conjugate in permeabilized tissue culture cells (*21*), while another showed inhibition of ICAM-1 expression in living cells and used a novel method to detect triplex formation at the endogenous gene target (*22*). One of the major problems with in vivo assessment of TFO-mediated gene regulation is the delivery of the TFO to the target gene within the cell. A number of significant cellular barriers have limited the in vivo application of TFOs. For example, the cell membrane must be traversed, cytoplasmic compartmentalization and degradation must be avoided, and the target must be accessible within the structured chromatin. Furthermore, displacement of the TFO by DNA processing and repair enzymes must be prevented. Transfection of a reporter gene bearing a preformed triple helix provides a simple method to study the stability of the triple helix in living cells and the effects of triplex formation on target gene expression or replication (*23*, *24*).

In an attempt to prevent triplex displacement within cells, DNA reactive agents can be appended to the ends of TFOs. Nitrogen mustards and other alkylating agents have previously been shown to stabilize TFO binding by covalently attaching the oligonucleotide to the DNA target (*25*−*28*). When conjugated to a TFO, nitrogen mustards were shown to lack sufficient DNA binding affinity to alkylate DNA except near the triple helix (*29*). Bifunctional nitrogen mustards, such as chlorambucil, can form monoadducts with individual guanines and cross-links at sites with adjacent guanines. Interstrand cross-links are formed preferentially at 5′ GNC rather than 5′ GC sites, and are thought to be especially cytotoxic in vivo (*30*−*33*). Although cross-links by TFO-nitrogen mustard conjugates would be expected at appropriate sites adjacent to the triple helix, nitrogen mustards tethered to a TFO form predominantly monoadducts, and only trace amounts of cross-links have been observed (*34*). Dual monoadducts by both chlorambucils in a bis-chlorambucil conjugate were needed to demonstrate TFO-directed cross-linking with this bifunctional nitrogen mustard (*25*). A HER-2/neu specific TFO conjugated at only the 5′ end to chlorambucil was capable of site-specific binding and DNA alkylation, but the DNA alkylation directed by the monoconjugated TFO was a substrate for nucleotide excision repair (NER) (*35*). This result was consistent with other reports that indicated that a single site of DNA damage directed by a TFO-psoralen conjugate was efficiently repaired in cells while triplex-directed psoralen cross-links at both ends of the triple helix were not (*36*). It has also been recently demonstrated that DNA distortion induced by the triple helix itself can be targeted by the NER pathway (*37*). In addition, abasic sites created by the spontaneous depurination of alkylated guanines can be repaired by base excision repair (BER), which has recently been implicated in the removal of nitrogen mustard DNA adducts (*38*−*40*). Although BER

has not been studied in the context of TFO-nitrogen mustard conjugates, spontaneous depurination may occur rapidly with guanine monoadducts, whereas the spontaneous depurination of both guanines in a cross-link is much slower. In one study, spontaneous depurination of nitrogen mustard monoadducts alleviated blockage of RNA polymerase elongation in vitro with a half-life of approximately 10 h, while transcriptional blockages were sustained at sites of interstrand cross-links (*41*).

The current study expanded upon our previous findings to design a TFO that can form a more stable triple helix within cells. First, the TFO was conjugated to a nitrogen mustard (phenylacetate mustard, or PAM) with a greater half-life in aqueous solution than chlorambucil (CHL) (*26*), providing more time for the oligonucleotide to locate its target before the alkylating agent is inactive. Second, the oligonucleotide was conjugated to PAM at both the 5′ and 3′ ends to allow covalent modification of both ends of the triplex target and potentially improve stability of the triple helix intracellularly. In addition, modification of the 3′ end of the TFO would be expected to inhibit oligonucleotide degradation by exonucleases (*42*, *43*). Finally, the oligonucleotide was modified by substitution of guanine residues with the pyrazolo-pyrimidine analogue of guanine (PPG) to alleviate self-alkylation by the nitrogen-mustard and potassium mediated inhibition of triplex formation by preventing self-association of the TFO (*8*, *29*).

Our current findings indicate that the bis-alkylating TFO is superior to a previously studied chlorambucil monoconjugate in its ability to suppress the activity of a reporter plasmid with a preformed triple helix. Suppression is maximal when phenylacetate mustard is conjugated to both ends instead of only one end due to greater retention of the triple helix within cells and inhibition of helicase and nuclease activities.

EXPERIMENTAL PROCEDURES

Oligonucleotide Synthesis. Unmodified oligonucleotides (ODN) were purchased from commercial sources and purified by denaturing polyacrylamide gel electrophoresis (PAGE) (see Figure 1C for sequence information). The ODN conjugates were synthesized by Epoch Biosciences (Bothell, WA) as previously described (*26*). Conjugates were stored in aliquots at −80 °C and thawed on ice. Guanine residues in all PAM-conjugated TFOs were substituted with a guanine analogue (PPG) (Figure 1B). The purine-rich TFOs were designed to bind antiparallel to the purine target strand, and are either unconjugated (GA28C), conjugated at one end to either chlorambucil or phenylacetate mustard (GA27−5′ CHL; GA25−5′ PAM; GA25−3′ PAM), or at both ends (GA25−bis-PAM). In the absence of a 3′ conjugate, the ODNs were capped with a 3′ hexanol moiety to help prevent exonuclease degradation.

Plasmid Constructs. The construct pGL3/HNP410 contains the HER-2/neu promoter from base −410 to +1 relative to the translation start site ligated into the XhoI and NcoI sites of pGL3 basic (Promega). The location of the HER-2/neu promoter triplex target sequence in its native promoter position is maintained at −245 to −218. The negative control plasmid used in transfection analysis contained the SV40 promoter driving luciferase expression (pGL3/SV40, Promega) and does not contain a triplex binding site. A renilla luciferase construct (pRL/SV40, Promega) was used as an internal control for transfection efficiency.

Triplex Reactions and In Vitro Binding Studies. Nondenaturing EMSA analysis was performed as previously described to determine the binding affinities of the TFOs for the triplex target sequence. Since the conjugated TFOs can covalently react with the target site, it is not possible to calculate a true dissociation constant. The concentration at which the duplex target is 50% triple stranded was used to calculate the approximate K_d so that the relative binding affinities of the TFOs could be compared (*44*). A 36-base pair end-labeled HER-2/neu duplex target sequence was incubated with increasing TFO concentrations at 37 °C for 24 h. Triplex reactions were performed using 0.01 μM target in 1× TBM (90 mM Tris pH 7.4, 90 mM borate, 10 mM $MgCl_2$).

Denaturing EMSA was performed to determine the percent of covalent adducts formed by GA25−bis-PAM. The 36-base pair duplex target was end-labeled on the purine or pyrimidine-rich strand and incubated with increasing TFO concentrations at 37 °C for 4 h. After triplex formation, reactions were denatured in formamide loading buffer at 90 °C for 1 min and resolved on a 10% denaturing polyacrylamide gel.

Piperidine cleavage was performed as described previously (*35*). A 250-base pair PstI/XmaI fragment of the pGL3/HNP410 plasmid was used to generate four different end-labeled templates, 5′ versus 3′ end top strand labeled, and 5′ vs 3′ end bottom strand labeled. Triplex formation was performed by incubating 0.03 μM of labeled promoter fragment with 1 μM TFO in a final volume of 10 μL 1× TBM, which results in 100% triplex formation as determined by EMSA analysis. Triplex mixtures were incubated at 37 °C for the times indicated. Reactions without TFO were performed to rule out nonspecific cleavage of the radiolabeled template by piperidine. Maxam−Gilbert G-reactions were performed to identify alkylated guanine residues (*45*).

Transient Transfection Analysis. Triplex formation was induced by incubating 0.02 μM HER-2/neu promoter luciferase plasmid (pGL3/HNP410) in the presence of 2 μM TFO for 4 h at 37 °C in 1× TBM. Unbound TFO was removed using a 1× TBM equilibrated Chromaspin-100 column (Clontech) prior to transfection. HeLa, NCI-H23, and NCI-H522 cells were obtained from the American Type Culture Collection (ATCC). XP12BE cells were obtained from the Corriell Cell Repository. Cells were cultured as recommended by the suppliers. A total of 2 μg of the triple helix containing plasmids and 20 ng of the internal control plasmid (pRL/SV40) were transfected via TransIT-LT1 (Mirus; Madison, WI) into 12-well dishes containing the cell lines in log phase. After transfection, cells were washed twice in phosphate buffered saline and lysed in 1× passive lysis buffer (Promega). Cell lysates were then analyzed for luciferase activity and normalized for transfection efficiency using Promega's Dual Luciferase assay. All experiments were repeated three times in duplicate wells. Luciferase activity from plasmid without TFO treatment was designated as 100% promoter activity.

Southern Blot Protection Assay. A total of 5 μg of triplex containing plasmid (pGL3/HNP410) was transfected into six-well dishes. Cells were harvested at the specified time post-

transfection, and plasmids were isolated using the Wizard genomic DNA isolation kit (Promega). The DNA was BseRI digested, then isolated on a 1% agarose gel and transferred to nylon membrane. A 300-bp PstI/ApaI fragment of the HER-2/neu promoter was internally radiolabeled by random priming and used for membrane probing by standard high stringency Southern analysis (*45*). Protection from BseRI digestion due to triplex formation was quantitated by Eagle-Eye densitometry analysis. BseRI fragments of the endogenous (genomic) HER-2/neu promoter differ in size from the BseRI fragments of the pGL3/HNP410 plasmid and are not detected under the conditions employed in this assay.

Helicase Studies. Helicase unwinding of triplex DNA was performed as previously described with slight modifications (*46*). The HER-2/neu promoter was synthesized as a tailed duplex with a 5′ thymine rich overhang to generate the loading strand while limiting secondary structure formation. The tailed duplexes were end-labeled on the loading strand using T4 polynucleotide kinase and PAGE purified. Triplex reactions were performed in the standard 1× TBM buffer for 4 h prior to incubation with Dda helicase for 15 min. Recombinant T4 Dda helicase was prepared as previously described (*47*, *48*). Triplex reactions (1 nM) were incubated with helicase in the recommended unwinding buffer plus a 10-fold excess of unlabeled loading strand to prevent strand reassociation. Reactions were terminated by adding glycerol loading buffer and loaded immediately on a native 16% 1× TBM−PAGE gel.

Nuclease Sensitivity Assays. HeLa whole cell extracts (WCE) were isolated as described (*49*). A total of 1 μM TFO was incubated with 10 μg of HeLa WCE in a final reaction volume of 10 μL 1× PBS. In the cell culture media study, 1 μM specified TFO was incubated in 10 μL of RPMI + 10% FBS for the time indicated. Reactions were frozen immediately at −80 °C until thawed in formamide loading buffer and heated to 90 °C for 2 min before loading on a 16% denaturing PAGE gel. Oligonucleotides with free 5′ ends (GA28C and GA25−3′ PAM) were end-labeled with γATP using T4 PNK prior to incubation with media or WCE. Those oligonucleotides with modified 5′ ends (GA25−5′ PAM and GA25−bis-PAM) were incubated with media or WCE, and were detected after electrophoresis by transfer onto positively charged nylon membranes and probed with an end-labeled complementary oligonucleotide using standard Southern blot methods (*45*).

RESULTS

We have previously described the site-specific binding and alkylation at the HER-2/neu promoter triplex target site by a TFO conjugated to chlorambucil at the 5′ end (*35*). Despite the ability of this TFO to efficiently bind and alkylate the triplex target sequence in vitro, it was not capable of inhibiting HER-2/neu transcription in mammalian cancer cells using a reporter plasmid with a preformed triple helix in transient transfection assays. In the current study, TFOs were conjugated to nitrogen mustards at both ends in an attempt to stabilize triplex formation by introducing dual covalent adducts. This bis-conjugate was compared to TFOs of identical sequence conjugated at only the 5′ or 3′ end (monoconjugates), as well as the unconjugated TFO and the 5′ chlorambucil conjugated TFO.

TFOs and Triplex Target Sequences. The HER-2/neu promoter triplex target sequence is illustrated in Figure 1A. It is a 28-base pair purine/pyrimidine-rich tract juxtaposed between two important core promoter regulatory elements, the CCAAT (−249 to −253) and TATAA (−201 to −205) boxes. The sequences and binding orientations of the TFOs and locations of the nitrogen-mustard conjugates are denoted beneath the target sequence. The TFOs are purine-rich and bind antiparallel to the purine strand of the duplex target. The HER-2/neu specific TFOs GA25−5′ PAM and GA25−3′ PAM were conjugated at only one end to PAM (referred to as monoconjugates), while GA25−bis-PAM was conjugated at both ends (bis-conjugate). The 5′ TFO conjugates have a hexanol residue on the 3′ end to prevent intracellular degradation due to 3′ exonuclease activity. Guanine residues in the PAM-conjugated TFOs were substituted with a pyrazolopyrimidine analogue of guanine (PPG) to reduce the potential for TFO self-alkylation and self-association (Figure 1B).

Figure 1C illustrates the structures of the nitrogen mustard conjugates, chlorambucil (CHL) and phenylacetate mustard (PAM). PAM is a bifunctional nitrogen mustard composed of two chloroethylamine groups attached to phenylacetic acid, while the chloroethylamine groups of chlorambucil are attached to benzene butanoic acid. The chloroethylamine groups (highlighted) of the nitrogen mustard spontaneously form highly reactive aziridinium ion intermediates in aqueous solution. This intermediate can then interact with nearby nucleophiles, such as the N7 of guanine, to covalently alkylate DNA. In the absence of a nearby nucleophile, the highly reactive aziridinium intermediate can also react with water, resulting in hydrolysis and inactivation of the reactive group. The shorter acetic acid group on PAM slows the formation of the aziridinium ion intermediate and imparts a longer half-life in aqueous solution than chlorambucil (57 versus 27 min) (*26*).

In Vitro TFO Binding and Alkylation Efficiencies. Nondenaturing electrophoretic mobility shift analysis (EMSA) was performed to determine the binding affinities of the TFOs for the duplex DNA target sequence. A representative EMSA is illustrated in Figure 2A with increasing concentrations of the bis-conjugate (GA25−bis-PAM) incubated with double-stranded (ds) promoter target (0.01 μM), and the approximate dissociation constants for all TFOs are given in Table 1. The K_d of the unconjugated TFO (GA28C) was 0.015 μM and did not significantly change regardless of the number or location of the nitrogen-mustard conjugates or by shortening the TFO by 1−3 nucleotides for optimal placement of the nitrogen mustard relative to its target guanine base. The binding of the bis-conjugate TFO was nearly maximal at 4 h with an approximate K_d of 0.025 μM, compared to 0.020 μM for prolonged incubation.

Alkylation efficiency at each target guanine was determined by piperidine cleavage analysis. Sites of TFO-directed alkylation can be visualized by converting guanine adducts to single-strand DNA breaks via piperidine and heat, and a comparison of full-length template versus cleavage products can be used to determine the amount of site-specific alkylation. Figure 2B illustrates representative piperidine cleavage experiments with the bis-conjugate when the promoter template is labeled at the 5′ end of the top strand (lanes 1−6), versus the 3′ end of the top strand (lanes 7−12).

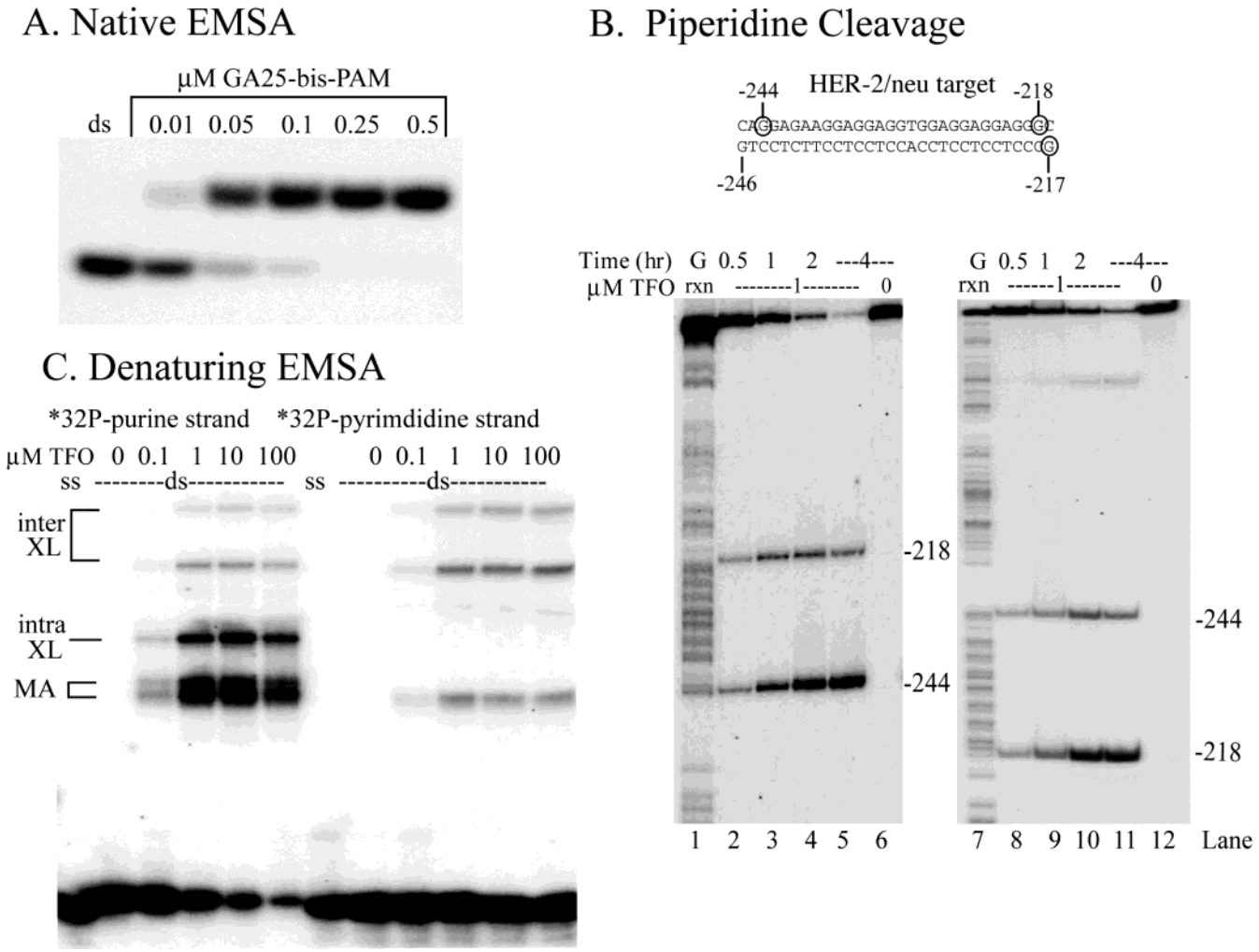

FIGURE 2: In vitro binding and alkylation efficiencies. (A) Representative native EMSA using the bis-conjugate TFO. (B) Representative piperidine cleavage gels demonstrating bis-conjugate TFO alkylation. The template in gel 1 was labeled on the 5′ end of the top strand to detect G-244 alkylation. The template in gel 2 was labeled on the 3′ end of the top strand to detect G-218 alkylation. Lanes 1 and 7 are HER-2/neu promoter Maxim-Gilbert G-reactions used to identify cleaved guanine residues. Lanes 2−5 and 8−11 are templates incubated with 1 μM TFO for increasing amounts of time. Lanes 6 and 12 are control templates without TFO. (C) Denautring EMSA demonstrating ability of bis-conjugate TFO to cross-link the duplex target sequence.

Table 1: Summary of in Vitro TFO Binding Properties[a]

		target bases				cross-links	
TFO	K_d (μM)	−217	−218	−244	−246	intra-strand	inter-strand
GA25−bis-PAM	0.020	25	70	70	<5	30	10
GA25−5′ PAM	0.010	25	70	N/A	N/A	N/A	
GA25−3′ PAM	0.010	N/A	N/A	70	0		
GA27−5′ CHL	0.012	0	70	N/A	N/A		
GA28C	0.015	N/A	N/A	N/A	N/A		

[a] ND = not determined, NA = not applicable.

The alkylation efficiency of the dual alkylating bis-conjugate can only be measured at the target guanine closest to the labeled end of the probe. Alkylation at G-244 (lane 5) and G-218 (lane 11) were both approximately 70% maximally. Alkylation of at least one of the two top strand target guanines was 90−100%, as indicated by the near absence of full-length probe over time. Piperidine cleavage assays with the bottom (pyrimidine) strand labeled showed that alkylation at G-217 was maximal at 25%, while G-246 alkylation levels were less than 5%. There was no alkylation detected at nontarget guanines, supporting the previous observation that when tethered to an oligonucleotide, the nitrogen mustard lacks sufficient DNA binding affinity to alkylate DNA except near the triple helix (*29*). Alkylation was maximal at 4 h (approximately four half-lives of PAM), and reactions allowed to proceed for 24 h showed little further alkylation of the target guanines. On the basis of the EMSA and piperidine cleavage results, triplex reactions for the remainder of the experiments were incubated for 4 h.

Denaturing EMSA was performed to estimate the efficiency of cross-link formation by the bis-conjugate (Figure 2C). Since the bis-conjugate has a bifunctional nitrogen mustard at both ends of the TFO, interstrand cross-links could form at G-217/G-218 or G-217/G-244 and an intrastrand cross-link could form at G-218/G-244, since alkylation at G-246 is negligible. Interstrand cross-links (XLs) are identified in the EMSA illustrated in Figure 2C as the two complexes of slowest mobility, with identical complexes regardless whether the duplex is labeled on the purine and pyrimidine strand. Individual monoadducts are the complexes with the most rapid mobility, and the intrastrand cross-link yields a complex of intermediate mobility for the purine strand only. Interstrand cross-links formed inefficiently

(10%), while intrastrand cross-link formation on the purine strand occurred in 30% of the triple helix formed by GA25−bis-PAM. These data are in general agreement with previous observations that interstrand cross-links by TFO-nitrogen mustard conjugates are much less efficient than monoadducts, even if an appropriate cross-link target is adjacent to the triple helix (*26*). On the basis of the alkylation efficiency at each guanine by piperidine cleavage analysis, cross-link efficiency appears to be lower than expected by the denaturing EMSA. Intrastrand cross-links are predicted to occur at a rate of approximately 50%, the product of 70% alkylation at each guanine, based on the piperidine cleavage assay.

Table 1 summarizes the in vitro binding properties of the TFO-nitrogen mustard conjugates. The monoconjugates alkylated the individual target guanines with approximately the same efficiency as the bis-conjugate. The in vitro binding studies demonstrate the potential for the bis-conjugate to improve triple helix stability intracellularly due to its ability to alkylate at least one target guanine with nearly 100% efficiency and to introduce intra- or interstrand cross-links with at least 40% efficiency.

Inhibition of Plasmid-Directed HER-2/neu Promoter Activity Intracellularly. Transfection analysis with a preformed triple helix was performed to determine whether the TFO would be capable of inhibiting HER-2/neu promoter activity intracellularly (Figure 3). To evaluate the role of single versus dual alkylation, the bis-conjugate and otherwise identical 5′ and 3′ monoconjugates were evaluated. Three different cell lines were tested that arise from different tissue sources and express HER-2/neu at different levels from a normal copy number of the HER-2/neu gene. HeLa cells are human cervical cancer cells with low HER-2/neu expression. NCI−H23 are nonsmall cell lung cancer cells (NSCLC) that express low levels of HER-2/neu, while NSCLC NCI−H522 highly overexpress HER-2/neu due to transcriptional activation (*50*). Triplex formation took place on a supercoiled plasmid containing the HER-2/neu promoter driving expression of a luciferase reporter gene (pGL3/HNP410). Unconjugated GA28C and GA27−5′CHL were unable to inhibit promoter activity in any cell line, even though the concentrations tested were known to bind (unconjugated) and alkylate (monoconjugated) the triplex target efficiently in vitro. The bis-conjugated TFO was able to suppress promoter activity in all three cell lines by 60−70%. In contrast, both monoconjugates were capable of suppressing HER-2/neu promoter activity by only approximately 20%. These studies were done with 2 μM TFO, representing a 100-fold molar excess to the concentration of the target plasmid, to drive rapid triplex formation for maximal alkylation efficiency. In addition, triplex formation with 0.2 μM of the bis-conjugate, representing a 10-fold molar excess of TFO to plasmid DNA, suppressed promoter activity by approximately 50%. In piperidine cleavage assays, the lower concentration of GA25−bis-PAM had a slightly lower alkylation efficiency (data not shown). An SV40 driven luciferase construct (no TFO target sequence) treated with the same oligonucleotides showed no effect on luciferase expression, demonstrating the specificity for HER-2/neu promoter suppression. Interestingly, the level of promoter suppression by the bis-conjugate did not appear to depend on cell type or the level of endogenous HER-2/neu expression.

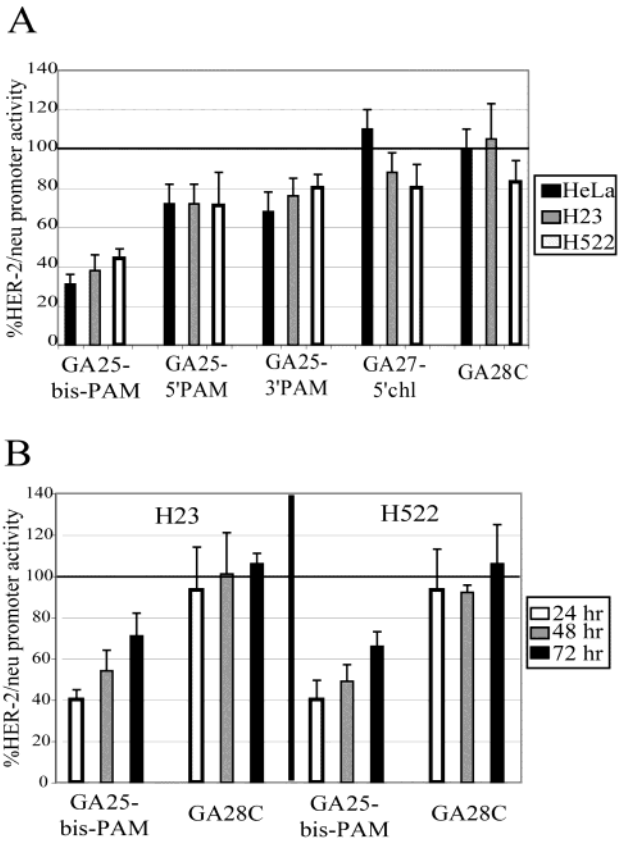

FIGURE 3: Transient transfection analysis. (A) A HER-2/neu promoter driven luciferase plasmid was incubated with the indicated TFOs and transfected into HeLa, NCI−H23, or NCI−H522 cells. Cells were analyzed for luciferase activity after 24 h. Untreated plasmid was defined as 100% promoter activity, and treatments are given as a percentage of full promoter activity. Experiments were performed in triplicate and average values with standard deviation are depicted. (B) Time course analysis demonstrating the effects of GA25−bis-PAM and GA28C (negative control) on promoter activity up to 72 h.

To determine triplex stability over time, cells were analyzed for HER-2/neu promoter activity 24, 48, and 72 h post-transfection with triple-helix containing plasmids (Figure 3B). The unconjugated TFO (GA28C) had no effect on promoter activity at any time point and was used as a negative control. In both NSCLC cell lines, the bis-conjugate suppressed promoter activity by approximately 60% at 24 h, 50% at 48 h, and 30% at 72 h, suggesting the removal of the triple helix over time. In the above studies, only the bis-conjugate was capable of significantly suppressing HER-2/neu promoter activity, indicating that alkylation at both ends of the triple helix may be required to stabilize the triple helix intracellularly or that alkylation at both ends of the triple helix is required to effectively prevent transcription factor binding and transcription initiation.

Intracellular Retention of Preformed Bis-Adduct Triple Helix. In an attempt to determine if dual alkylation stabilizes the triple helix in cells, a restriction enzyme protection assay was used to determine the amount of triple helix retained after plasmid transfection into HeLa cells (Figure 4). The HER-2/neu promoter contains three sites for cleavage with the restriction enzyme BseRI within the triplex target sequence. There are also sites 3400 bp upstream of the triplex target and 800 bp downstream in the pGL3 vector. In the absence of triplex formation, BseRI digestion will result in

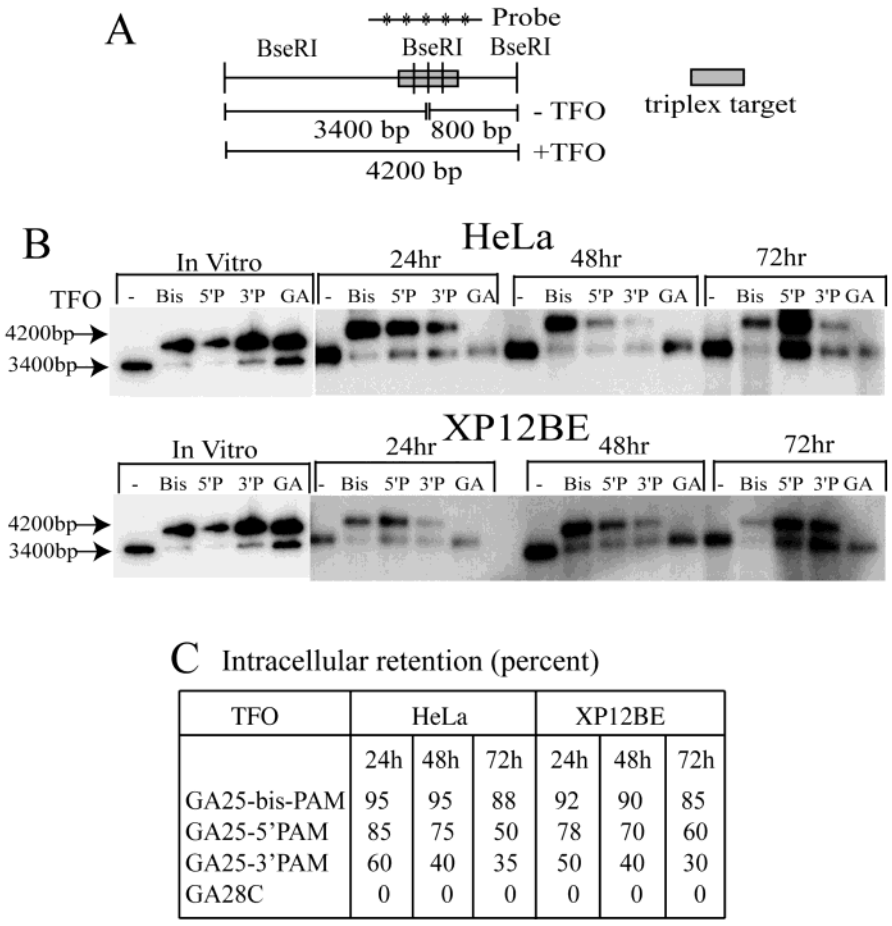

C Intracellular retention (percent)

TFO	HeLa			XP12BE		
	24h	48h	72h	24h	48h	72h
GA25-bis-PAM	95	95	88	92	90	85
GA25-5'PAM	85	75	50	78	70	60
GA25-3'PAM	60	40	35	50	40	30
GA28C	0	0	0	0	0	0

FIGURE 4: Intracellular retention of triple helix containing plasmids as determined by Southern blot assays. (A) Schematic of the HER-2/neu promoter indicating BseRI restriction sites. In the absence of TFO (-TFO) 2 restriction fragments are obtained, while if triple helix is present (+TFO), one 4200-bp fragment is obtained. (B) Demonstration of triplex containing plasmids and their susceptibility to BseRI digestion in vitro and after transfection into HeLa cells (top panel) or XP12BE cells (bottom panel)(P = PAM, GA = GA28C). Plasmid DNA was recovered 24−72 h post-transfection for Southern blot analysis. (C) Percent of triple helix retained as determined by restriction enzyme protection and Southern blot assays in NER competent (HeLa) versus NER-deficient (XP12BE) human cancer cells.

two fragments of 3400 and 800 bp pairs; however, triplex formation can block the BseRI recognition sites within the triplex target, resulting in a single fragment of 4200 base pairs. These fragments can be detected and quantified by Southern blot analysis with a probe for the HER-2/neu promoter (Figure 4A).

Prior to transfection, all TFOs protected 95−100% of the internal BseRI restriction sites in vitro (Figure 4B). These same plasmids were transfected into HeLa cells, and plasmid DNA was isolated at 24, 48, and 72 h intervals for BseRI digestion and Southern analysis (Figure 4B, top panel). The triple helix formed by the bis-conjugate was very stable in HeLa cells, and the majority of this triplex was retained even after 72 h with very little loss. The triple helices formed by the monoconjugates were less stable in HeLa cells and were partially removed over time. Approximately 50% of the triple helix formed by the 5′ monoconjugate was removed after 72 h. This triple helix was more stable than the triple helix formed by the 3′ monoconjugate, and the majority (65%) of the latter triplex was lost after 72 h in HeLa cells. It is likely that the ability of the 5′ PAM conjugate to form an additional adduct with a guanine (G-217) on the pyrimidine-rich strand (25% alkylation efficiency, see Figure 2) and an interstrand cross-link, albeit inefficiently (G-217/G-218 interstrand cross-links are estimated to occur in at least 5% of the triplexes by denaturing EMSA, not shown), accounts for the greater intracellular stability compared to the 3′ conjugate, which is capable of forming only a single adduct with a guanine on the purine rich strand. The unconjugated TFO was completely removed intracellularly by 24 h.

Previous studies using in vitro repair assays demonstrated that GA27−5′CHL induced guanine adducts were substrates for nucleotide excision repair (NER) (*35*). Triplex-directed DNA adducts have previously been shown to be substrates for the more specific transcription coupled repair (TCR), a specific type of NER (*17*). However, because the predominant adducts formed by the TFO−PAM conjugates are with guanines on the nontemplate strand upstream of the major transcription start site, it is unlikely that TCR plays a significant role in removal of these adducts. To determine the effects of NER on the PAM-stabilized triple helices, intracellular triple helix retention levels were compared between NER competent HeLa cells and NER-deficient XP12BE cells (Figure 4B, bottom panel). Interestingly, there was a similar trend in the intracellular retention of the PAM-stabilized triple helices in NER-proficient versus deficient cells over 72 h, indicating that NER is not the only process that can remove the triple helix and guanine adducts intracellularly, and suggesting a possible role for depurination and BER in the removal of the guanine adducts in both cell types.

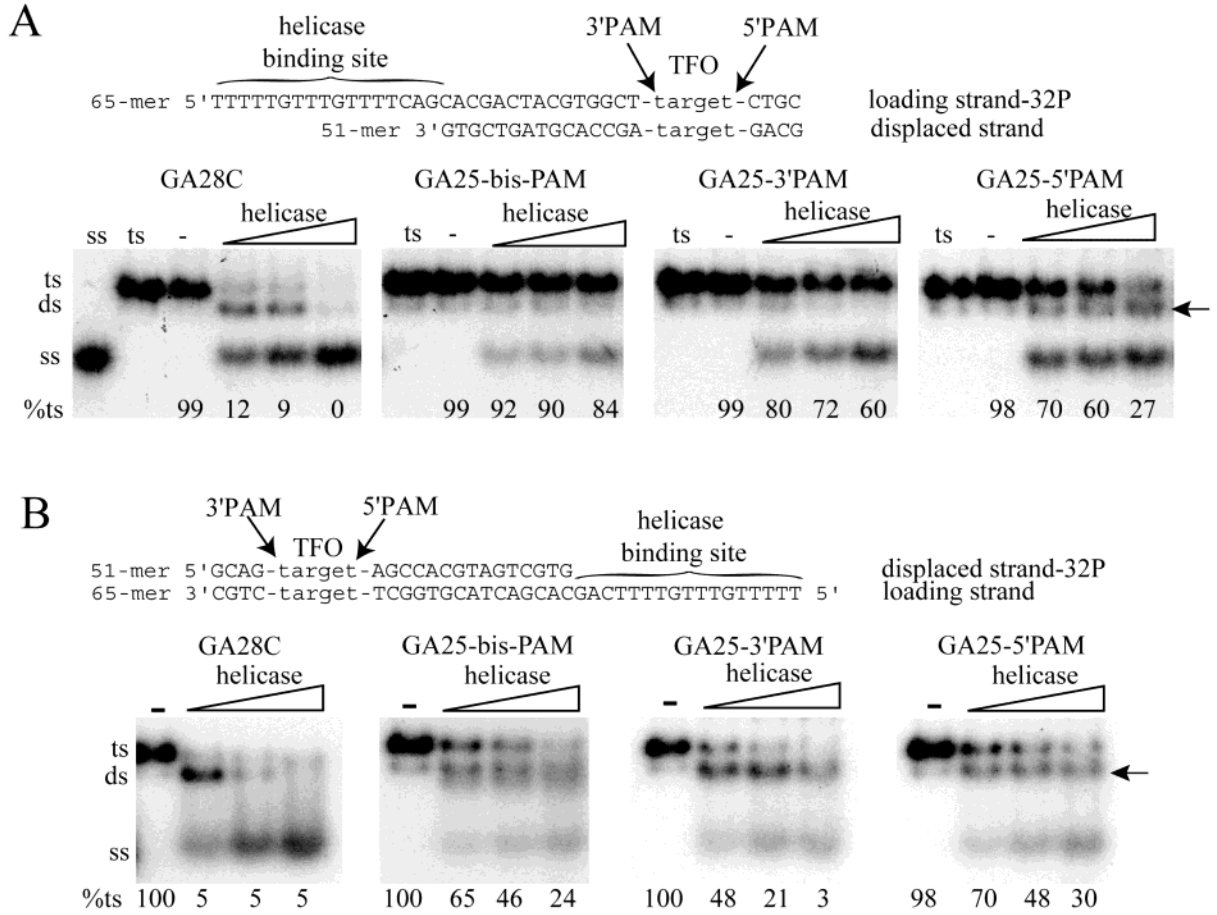

FIGURE 5: Triple-helix susceptibility to helicase activity. (A) Upper schematic demonstrates the duplex target sequence. The purine-rich promoter strand has a single-stranded overhang for helicase binding, and is termed the loading strand. The target sequence was indicated in Figure 1. The alkylation sites for the 5′ PAM versus the 3′ PAM conjugates are noted, as the TFO binds antiparallel to the purine strand. In the helicase assays with various TFOs, the triple-stranded DNA was either untreated (ts), incubated in unwinding buffer without helicase (−), or incubated with increasing concentrations of helicase (open triangle) from 0.2 to 20 nM. Double-stranded (ds) and single-stranded (ss) DNA mobilities are indicated. (B) Schematic of the target sequence, and representative helicase assays using the pyrimidine-rich strand as the helicase loading strand, and the purine-rich strand as the radiolabeled strand. The helicase dissociation product likely representing the purine-rich strands of the duplex and the covalently bound TFO (arrow) is discussed in the text.

It is also important to note that the majority of triple helices formed by both the 5′ and the 3′ PAM conjugates are retained at 24 h (85 and 60%, respectively), a time point at which triple helix formation by the monoconjugates shows only minimal suppression of HER-2/neu driven luciferase activity. To explain this dichotomy, we hypothesize that the triple helices formed by the monoconjugates are more susceptible to helicase unwinding, even though they are mostly retained within cells as indicated by the Southern blot assay. Helicase activity may unwind the triple helix up to the point of DNA alkylation without removing the guanine adduct, resulting in the TFO remaining attached to the plasmid only by the covalent adduct but incapable of preventing HER-2/neu transcription in cells.

In Vitro Helicase Susceptibility. Triplex formation with the bis-conjugate may suppress promoter activity by inhibiting common intracellular enzymatic activities that act on DNA, such as helicase unwinding and nuclease degradation. DNA helicases from a variety of sources have generally been shown to unwind triplex DNA, although unwinding by SV40 large T antigen has been able to unwind and be inhibited by a triple helix (*46*, *51*−*55*). To evaluate the ability of the TFO−PAM conjugates to prevent DNA unwinding, T4 Dda helicase was used to unwind the HER-2/neu promoter in vitro. T4 Dda helicase is a 5′ to 3′ helicase that is homologous to human DNA helicase B, which is believed to be required for human chromosomal DNA replication (*47*, *56*). Dda is known to be capable of efficiently unwinding a triple helix, can readily displace streptavidin from a biotinylated oligo at rates much faster than other helicases, and was selected to provide a stringent test of the stability of the covalently bound TFOs (*46*, *57*).

Most helicases initiate unwinding in vitro at a region of single-stranded DNA adjacent to the duplex DNA (*51*). For these studies, tailed duplexes containing a 5′ overhang were employed, and the strand containing the overhang is referred to as the loading strand while the complementary strand is referred to as the displaced strand (see sequences in Figure 5). Figure 5A illustrates EMSAs following treatment of various triple helices with Dda helicase when the purine-rich strand is the loading and radiolabeled strand. The noncovalent triple helix with GA28C was efficiently converted entirely to single-stranded DNA by increasing concentrations of Dda helicase. The triple helix with dual covalent adducts with GA25−bis-PAM showed the greatest stability with 92 to 85% retention levels over increasing helicase concentrations, and the predominant dissociation product was single-stranded DNA. The triple helices with

single covalent adducts formed by GA25−5′ PAM or GA25−3′ PAM were more susceptible to dissociation by recombinant helicase. At the highest helicase concentration (20 nM), 60% of the triple helix formed by GA25−3′ PAM remained, again converted entirely to single-stranded DNA. Only 25% of the triple helix formed by GA25−5′ PAM remained after treating with the highest helicase concentration, with 30−40% of the triple helix converted to single-stranded DNA and 40% to an intermediate complex of similar mobility as double-stranded DNA (noted by the arrow). Time course analysis (not shown) indicated that unwinding of the various triple helices did not change over prolonged incubation with the helicase protein (5 min to 1 h), indicating that maximal unwinding occurs rapidly. Overall, the stability of the triple helices to 5′ to 3′ helicase activity was bis-PAM > 3′ PAM > 5′ PAM > GA28C.

The intermediate complex formed after helicase unwinding of the triple helix formed by GA25−5′ PAM (denoted by arrow) was isolated from the gel and subjected to piperidine cleavage, and was 95% cleavable with piperidine (not shown). Piperidine susceptibility and the size of the cleaved fragment indicates the persistence of the guanine adduct (or an abasic site) at the site of alkylation (G-218) on the purine-rich loading strand. In contrast, the single-stranded DNA fragment was not susceptible to piperidine cleavage. Thus, helicase activity dissociated the triple helix into the single-stranded displaced strand (pyrimidine rich) in the absence of a covalent adduct, since in all instances the amount of single-stranded DNA resulting from helicase unwinding is proportionate to the amount of unalkylated DNA as determined in piperidine cleavage assays. Helicase activity was able to dissociate the displaced strand but not the covalently bound 5′ conjugate from the loading (purine rich) strand, which accounts for the piperidine susceptibility of the intermediate complex (TFO plus loading strand).

The apparent greater stability of the 3′ conjugate versus the 5′ conjugate against helicase activity translocating from the 5′ end of the target may be explained by the amount of double-stranded DNA distal (3′) to the covalent adduct (see Figure 5A schematic). In the case of the 3′ PAM TFO, the Dda helicase may unwind the duplex up to the point of the proximal covalent adduct which prevents further 5′ to 3′ helicase translocation, and the long (30 base pair) region of downstream DNA remains associated. In contrast, in the case of the 5′ PAM TFO, helicase can unwind the duplex and triplex up to the point of the downstream covalent guanine adduct, which leaves only four base pairs of duplex DNA associated, and this unstable short duplex dissociates into the loading strand plus TFO intermediate (arrow) and unlabeled displaced strand.

When the pyrimidine strand was used as the loading strand (Figure 5B), nearly all of the triple helices formed by the PAM conjugates were converted to the TFO-purine strand covalent complex (arrow) and single-stranded DNA, and the relative amount of each is again proportionate to alkylation efficiency. A small amount of triple helix remains associated in the case of the 5′ PAM and bis-PAM triple helices (25%), proportionate to the amount of alkylation observed at G-217 on the pyrimidine-rich strand in the piperidine cleavage assays.

The greater stability against helicase activity of the triple helix formed by the bis-conjugate reflects its overall higher alkylation efficiency of 90−100% of at least one of the target guanines. These data indicate that the covalent TFO-guanine adducts are capable of blocking Dda helicase translocation; however, a TFO covalently bound at only one end of the triple helix may be unwound up to the point of the adduct. In these studies, we only evaluated 5′ to 3′ helicase activity; it is likely that the triple helix formed by the 3′ PAM conjugate would be similarly unwound by 3′ to 5′ helicases. The ability of the bis-conjugate to resist helicase unwinding may account for the improved stability of the bis-conjugated triple helix in cells and its ability to suppress HER-2/neu promoter activity.

Nuclease Sensitivity of TFO Conjugates. Since a TFO covalently bound at only one end of the triple helix may be unwound up to the point of the adduct, this may expose the free end of the TFO to nuclease degradation. Therefore, the TFOs were exposed to the nucleases present in the cell culture model, namely, those found in serum and cellular protein extracts. TFOs with free 5′ ends were end-labeled (Figure 6A), while those with 5′ end modifications were transferred to nylon membrane for complementary oligonucleotide probing (Figure 6B) after they were exposed to HeLa whole cell extracts (WCE). Figure 6C is a graphical representation of the percent of full-length TFO over time in HeLa WCE, and panel D represents TFO half-lives in both HeLa WCE and cell culture media with 10% serum. The unmodified TFO (GA28C) was rapidly degraded, with a half-life of 20 min in HeLa WCE and 30 min in serum-containing culture media. The bis-PAM and 3′ PAM TFOs were equally stable when exposed to both sources of nucleases, with half-lives of 4 h in HeLa WCE and 24 h in serum-containing culture media, while the 5′ PAM TFO was slightly less stable against both sources of nuclease activity. The 5′ PAM conjugate is modified with hexanol at the 3′ end to help prevent 3′ to 5′ exonuclease activity. These data indicate a PAM conjugate at the 3′ end of the oligonucleotide is a slightly better inhibitor of 3′ exonuclease activity than the 3′ hexanol derivative. These data are also in agreement with previous observations that suggest that the predominant nuclease activity that degrades oligonucleotides in the cell culture model is 3′ to 5′ exonuclease activity that can be largely prevented by modification of the 3′ end of the oligonucleotide (*58*)

DISCUSSION

This study describes the effective inhibition of HER-2/neu promoter expression by a TFO conjugated at both ends to a DNA alkylating agent using a model system with a triple helix formed on a plasmid. We systematically demonstrated the requirements for triplex formation and retention on a target sequence in plasmid DNA both in vitro and in cell culture. Table 2 summarizes the in vitro and intracellular effects of the various TFOs to compare the ability of the TFOs to suppress promoter activity in cells with the TFO alkylation efficiency, intracellular retention of the triple helix, and stability against helicase and nuclease activity. The bis-conjugate was the only TFO that significantly inhibited HER-2/neu promoter activity. The decrease in reporter gene expression may reflect the approximate proportion of the triplex targets that contains interstrand and intrastrand cross-links. Intrastrand cross-links were demonstrated to occur on approximately 10% of the target sequences, and intrastrand

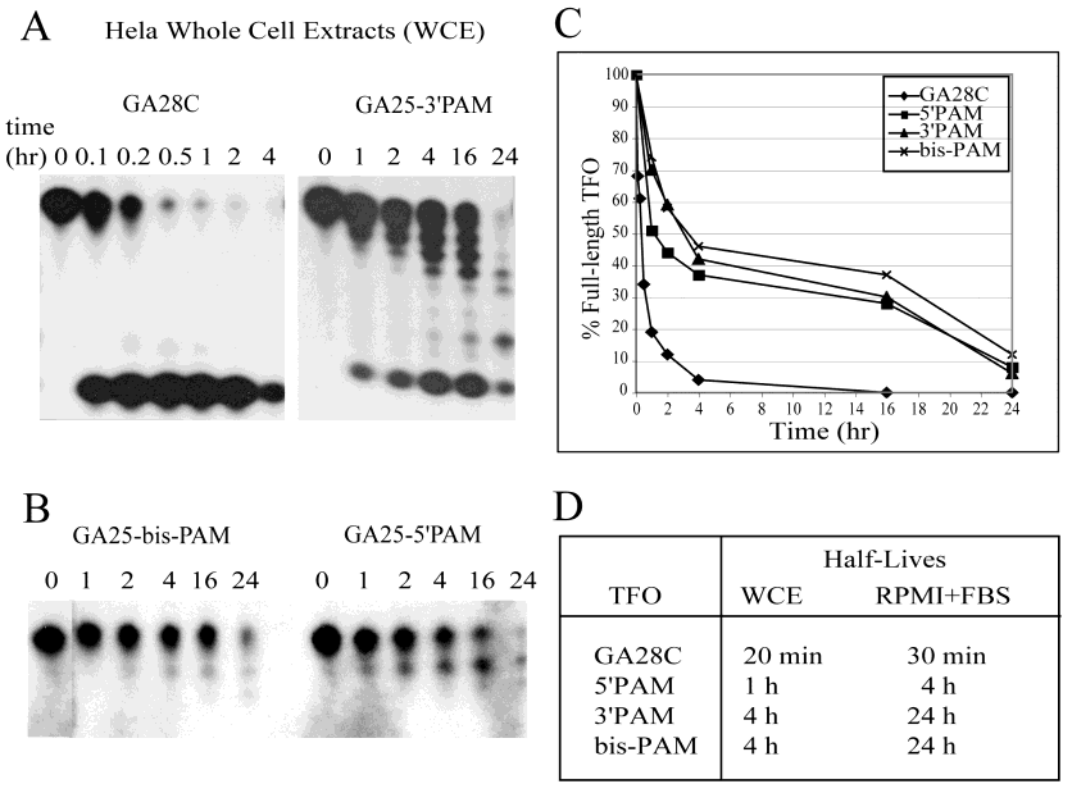

TFO	Half-Lives WCE	RPMI+FBS
GA28C	20 min	30 min
5'PAM	1 h	4 h
3'PAM	4 h	24 h
bis-PAM	4 h	24 h

FIGURE 6: Nuclease sensitivity of TFOs. End-labeled TFOs (A) or unlabeled TFOs detected with a radiolabeled complementary oligonucleotide (B) were incubated with 10 μg of HeLa whole cell extracts for increasing time points. (C) Graphical representation of the percent of full-length TFO over time of incubation with HeLa whole cell extracts. (D) Table indicates TFO half-lives in cell extracts and cell culture media.

Table 2: Summary of in Vitro and Intracellular Activities of TFOs[a]

TFO	% alkylation mono	dual	total	promoter suppression (%)	intracellular retention (%)	helicase susceptibility	nuclease susceptibility
GA25-bis-PAM	70	50	100	65	95	+	+
GA25−5′ PAM	70	NA	70	20	85	+++	++
GA25−3′ PAM	70	NA	70	20	60	++	+
GA27−5′ chl	70	NA	70	10	ND	ND	ND
GA28C	NA	NA	NA	0	0	++++	++++

[a] Susceptibility scale ranges from low (+) to high (++++). ND = not determined, NA = not applicable.

cross-links were found in 30−50% of the targets (depending on methodology), numerically similar to the approximately 60% suppression of reporter gene expression observed for the bis-conjugate. Thus, inhibition of gene expression by triplex-directed covalent adduct formation with the target sequence is greatly enhanced by a TFO capable of forming cross-links compared to only monoadducts. The triple helix formed by the bis-conjugate appeared highly stable within cells, and was not susceptible to helicase unwinding. The presence of a 3′ terminus modification with PAM also prevented nuclease degradation of the TFO. The triplexes formed by the mono-PAM conjugates had a minimal effect on promoter activity, were less stable in cells, and were removed by helicase proportionate to the amount of unalkylated DNA. We believe these studies demonstrate that TFOs conjugated at both the 5′ and 3′ ends with alkylating agents will be superior to unconjugated or monoconjugated TFOs in the regulation of gene expression. This conclusion is in accordance with data demonstrating that a TFO conjugated to psoralen on both ends was also less efficiently repaired within cells compared to a single adduct (*36*). Higher efficiency may be attained with other novel DNA binding agents that undergo hybridization triggered DNA adduct formation to improve adduct formation in cells, such as cyclopropapyrroloindole (CPI) (*59*) or pyrrolo-1,4-benzodiazepine (PBD) reactive moieties (unpublished observations) (*60*, *61*).

One likely reason that the bis-conjugate significantly suppressed promoter activity is due to its ability to inhibit helicase activity. It was previously shown that Dda helicase unwound triplex DNA with an efficiency comparable to that of double-stranded DNA (*46*). Dda and other helicases can dissociate streptavidin from a biotinylated oligonucleotide, indicating that as the enzyme translocates down the DNA it imparts a force on molecules blocking its path (*57*, *62*). Although the only helicase used in this study unwinds DNA with a 5′ to 3′ directionality, a 3′ to 5′ helicase has also been similarly shown to displace streptavidin from a biotinylated DNA substrate (*63*). Therefore, it is unlikely that an unmodified triple helix will efficiently inhibit common intracellular enzyme complexes that involve helicase unwinding, such as RNA and DNA polymerase complexes, and DNA repair complexes. Agents that covalently modify the loading strand of duplex DNA, such as the antitumor drug

CC-1065, can inhibit helicase unwinding (*64*). Similarly, we have previously demonstrated that to prevent RNA polymerase elongation through the HER-2/neu coding sequence, covalent modification of the template strand is required (*8*). Our present findings seem to indicate that DNA helicases can unwind the triple helix up to the point of the covalent adduct, so that covalent modification at one end of the triple helix will remain susceptible to unwinding by a helicase that traverses through the noncovalently attached end. Covalent modification at both ends of the triple helix will be needed to stabilize the triple helix and reliably prevent helicases from unwinding the triple helix in cells.

Regardless of TFO design, a 60−70% decrease may be the maximal promoter suppression attainable by targeting this region of the HER-2/neu promoter. Previous HER-2/neu promoter studies indicated that mutating bases adjacent to the triplex target inhibited binding of an *ets* family member (PU.1) and subsequently decreased promoter activity by at least 60% (*65*). Even if triplex formation occurs efficiently at this target sequence, there may be alternative mechanisms of promoter regulation that allows for gene expression. Transcription initiation in the HER-2/neu promoter can be controlled independently at two separate regions, one within the triplex target at an initiator-like element, and one just downstream at the TATAA box (*66*). Triplex formation may inhibit transcription initiation from the initiator-like sequence where it binds, but not completely inhibit initiation from the TATAA box. Inhibition of transcription by the TFO may be due to competition for transcription factor binding, such as PU.1, or due to triple helix formation and covalent adducts that distort the duplex and affect the overall promoter structure. The consistency of triple helix intracellular retention and promoter suppression levels between multiple cell lines with normal HER-2/neu gene copies and various protein expression levels indicates the level of HER-2/neu promoter activation, which can vary between cell lines, does not change TFO effectiveness. Nonetheless, a 60−70% decrease in promoter activity may result in a therapeutically relevant decrease in HER-2/neu protein expression. For example, a monoclonal antibody targeting the HER-2/neu gene product now represents modestly effective treatment for certain HER-2/neu overexpressing cancers, while the antiproliferative effects of monoclonal antibody treatment are associated with at most an 80% decrease in HER-2/neu receptor phosphorylation and only a modest decrease in receptor density due to receptor internalization in HER-2/neu overexpressing breast cancer cell lines (*67*, *68*). An alternative strategy to prevent gene transcription by TFOs involves blocking RNA polymerase elongation rather than initiation by targeting the transcribed region of a gene, a strategy that has met with recent success and also greatly increases the number of potential triplex target sequences (*22*, *69*). Furthermore, active transcription of the target gene increases the accessibility of the coding region to TFO binding, potentially providing a basis for selectively targeting tumor cells versus normal tissues based on the level of transcription of the target gene (*70*).

In these studies, we used a model system of a preformed triple helix in a transiently transfected plasmid to study several of the important requirements for the suppression of gene expression by triple helix formation. In this way, the effects of triplex formation on gene expression can be studied without the need to overcome the substantial cellular barriers that limit triple helix formation at endogenous gene targets. Presently, inefficient TFO delivery limits the ability to assess the effects of triplex formation and triplex directed covalent adduct formation on endogenous gene expression. Indeed, one recent report demonstrated that cationic lipid delivery of an I^{125} labeled TFO with or without a nuclear localization signal induced the intended double stand breaks in the target mdr1 gene with <5% efficiency (*71*). Endogenous targets in digitonin permeabilized cells and isolated nuclei have been successfully targeted by TFOs; however, neither method allowed assessment of target gene expression levels (*21*, *72*). Recently, Besch et al. demonstrated inhibition of ICAM-1 expression in living cells and used a novel method to detect triplex formation at the endogenous gene target (*22*); however, the method of detecting triplex formation did not allow for quantitation of target site binding by the TFO. The present studies underscore the continued need for an efficient method of TFO delivery that results in adequate concentrations of TFO that is freely available in the nucleus to bind to the endogenous gene target.

Gene targeted therapeutics remains appealing due to the limited number of DNA targets within a cell and the potential to interfere with erroneous gene expression at the earliest stage. While the present studies involved a model system of triplex formation in a reporter plasmid, we can conclude that the effects of TFO treatment on gene expression were indeed due to triplex formation and were correlated with the stability of the triple helix in cells. TFOs capable of covalent adduct formation with important cancer related genes remain promising for therapeutics, and would be of potential use in many types of human cancer. The positive findings presented here encourage us to further explore the ability of the bisalkylating TFO to locate and interact with the endogenous HER-2/neu promoter and suppress transcription initiation in living cells, a goal that will depend on an effective delivery method to achieve triplex-directed gene regulation in vivo.

ACKNOWLEDGMENT

We thank Dr. Laurence Hurley of the Arizona Cancer Center for critical review of this manuscript.

REFERENCES

1. Le Doan, T., Perrouault, L., Praseuth, D., Habhoub, N., Decout, J. L., Thuong, N. T., Lhomme, J., and Helene, C. (1987) *Nucleic Acids Res. 15*, 7749−7760.
2. Moser, H. E., and Dervan, P. B. (1987) *Science 238*, 645−650.
3. Praseuth, D., Guieysse, A. L., and Helene, C. (1999) *Biochim. Biophys. Acta 1489*, 181−206.
4. Vasquez, K. M., Narayanan, L., and Glazer, P. M. (2000) *Science 290*, 530−533.
5. Cooney, M., Czernuszewicz, G., Postel, E. H., Flint, S. J., and Hogan, M. E. (1988) *Science 241*, 456−459.
6. Durland, R. H., Kessler, D. J., Gunnell, S., Duvic, M., Pettitt, B. M., and Hogan, M. E. (1991) *Biochemistry 30*, 9246−9255.
7. Mouscadet, J. F., Carteau, S., Goulaouic, H., Subra, F., and Auclair, C. (1994) *J. Biol. Chem. 269*, 21635−21638.
8. Ebbinghaus, S. W., Fortinberry, H., and Gamper, H. B., Jr. (1999) *Biochemistry 38*, 619−628.
9. Ebbinghaus, S. W., Gee, J. E., Rodu, B., Mayfield, C. A., Sanders, G., and Miller, D. M. (1993) *J. Clin. Invest. 92*, 2433−2439.
10. Jardines, L., Weiss, M., Fowble, B., and Greene, M. (1993) *Pathobiology 61*, 268−282.
11. Kern, J. A., Schwartz, D. A., Nordberg, J. E., Weiner, D. B., Greene, M. I., Torney, L., and Robinson, R. A. (1990) *Cancer Res. 50*, 5184−5187.

12. Yu, D., Wang, S. S., Dulski, K. M., Tsai, C. M., Nicolson, G. L., and Hung, M. C. (1994) *Cancer Res. 54*, 3260−3266.
13. Agus, D. B., Bunn, P. A., Jr., Franklin, W., Garcia, M., and Ozols, R. F. (2000) *Semin. Oncol. 27*, 53−63.
14. Meric, F., Hung, M. C., Hortobagyi, G. N., and Hunt, K. K. (2002) *J Am. Coll. Surg. 194*, 488−501.
15. Noonberg, S. B., Scott, G. K., Hunt, C. A., Hogan, M. E., and Benz, C. C. (1994) *Gene 149*, 123−126.
16. Barre, F. X., Ait-Si−Ali, S., Giovannangeli, C., Luis, R., Robin, P., Pritchard, L. L., Helene, C., and Harel-Bellan, A. (2000) *Proc. Natl. Acad. Sci. U.S.A. 97*, 3084−3088.
17. Wang, G., Seidman, M. M., and Glazer, P. M. (1996) *Science 271*, 802−805.
18. Guieysse, A. L., Praseuth, D., Grigoriev, M., Harel-Bellan, A., and Helene, C. (1996) *Nucleic Acids Res. 24*, 4210−4216.
19. Grigoriev, M., Praseuth, D., Guieysse, A. L., Robin, P., Thuong, N. T., Helene, C., and Harel-Bellan, A. (1993) *Proc Natl. Acad. Sci. U.S.A. 90*, 3501−3505.
20. Ing, N. H., Beekman, J. M., Kessler, D. J., Murphy, M., Jayaraman, K., Zendegui, J. G., Hogan, M. E., O'Malley, B. W., and Tsai, M. J. (1993) *Nucleic Acids Res. 21*, 2789−2796.
21. Giovannangeli, C., Diviacco, S., Labrousse, V., Gryaznov, S., Charneau, P., and Helene, C. (1997) *Proc. Natl. Acad. Sci. U.S.A. 94*, 79−84.
22. Besch, R., Giovannangeli, C., Kammerbauer, C., and Degitz, K. (2002) *J. Biol. Chem. 277*, 32473−32479.
23. Guieysse, A. L., Praseuth, D., Giovannangeli, C., Asseline, U., and Helene, C. (2000) *J. Mol. Biol. 296*, 373−383.
24. Diviacco, S., Rapozzi, V., Xodo, L., Helene, C., Quadrifoglio, F., and Giovannangeli, C. (2001) *FASEB J. 15*, 2660−2668.
25. Kutyavin, I. V., Gamper, H. B., Gall, A. A., and Meyer, R. B. (1993) *J. Am. Chem. Soc. 115*, 9303−9304.
26. Reed, M. W., Lukhtanov, E. A., Gorn, V. V., Kutyavin, I. V., Gall, A. A., Wald, A., and Meyer, R. B. (1998) *Bioconjug. Chem. 9*, 64−71.
27. Vlassov, V. V., Gaidamakov, S. A., Zarytova, V. F., Knorre, D. G., Levina, A. S., Nikonova, A. A., Podust, L. M., and Fedorova, O. S. (1988) *Gene 72*, 313−322.
28. Brossalina, E. B., Demchenko, E. N., Vlassov, V. V., and Mamaev, S. V. (1991) *Antisense Res. Dev. 1*, 229−242.
29. Lampe, J. N., Kutyavin, I. V., Rhinehart, R., Reed, M. W., Meyer, R. B., and Gamper, H. B., Jr. (1997) *Nucleic Acids Res. 25*, 4123−4131.
30. Struck, R. F., Davis, R. L., Jr., Berardini, M. D., and Loechler, E. L. (2000) *Cancer Chemother. Pharmacol. 45*, 59−62.
31. Millard, J. T., Luedtke, N. W., and Spencer, R. J. (1996) *Anticancer Drug Des. 11*, 485−492.
32. Bauer, G. B., and Povirk, L. F. (1997) *Nucleic Acids Res. 25*, 1211−1218.
33. Povirk, L. F., and Shuker, D. E. (1994) *Mutat. Res. 318*, 205−226.
34. Reed, M. W., Wald, A., and Meyer, R. B. (1998) *J. Am. Chem. Soc. 120*, 9729−9734.
35. Ziemba, A., Derosier, L. C., Methvin, R., Song, C. Y., Clary, E., Kahn, W., Milesi, D., Gorn, V., Reed, M., and Ebbinghaus, S. (2001) *Nucleic Acids Res. 29*, 4257−4263.
36. Sandor, Z., and Bredberg, A. (1995) *FEBS Lett. 374*, 287−291.
37. Vasquez, K. M., Christensen, J., Li, L., Finch, R. A., and Glazer, P. M. (2002) *Proc. Natl Acad. Sci. U.S.A. 99*, 5848−5853.
38. Salmelin, C., Hovinen, J., and Vilpo, J. (2000) *Mutat. Res. 467*, 129−138.
39. McHugh, P. J., Gill, R. D., Waters, R., and Hartley, J. A. (1999) *Nucleic Acids Res. 27*, 3259−3266.
40. Brooks, N., McHugh, P. J., Lee, M., and Hartley, J. A. (1999) *Anticancer Drug Des. 14*, 11−18.
41. Masta, A., Gray, P. J., and Phillips, D. R. (1994) *Nucleic Acids Res. 22*, 3880−3886.
42. Eder, P. S., DeVine, R. J., Dagle, J. M., and Walder, J. A. (1991) *Antisense Res. Dev. 1*, 141−151.
43. Fisher, T. L., Terhorst, T., Cao, X., and Wagner, R. W. (1993) *Nucleic Acids Res. 21*, 3857−3865.
44. Basye, J., Trent, J. O., Gao, D., and Ebbinghaus, S. W. (2001) *Nucleic Acids Res. 29*, 4873−4880.
45. Sambrook, J. and Russell, D. W. (2001) in *Molecular Cloning, A Laboratory Manual*, Cold Spring Harbor Laboratory Press, Cold Spring Harbor, NY.
46. Maine, I. P., and Kodadek, T. (1994) *Biochem. Biophys. Res. Commun. 204*, 1119−1124.
47. Raney, K. D., and Benkovic, S. J. (1995) *J. Biol. Chem. 270*, 22236−22242.
48. Hacker, K. J., and Alberts, B. M. (1992) *J. Biol. Chem. 267*, 20674−20681.
49. Wood, R. D., Robins, P., and Lindahl, T. (1988) *Cell 53*, 97−106.
50. Schneider, P. M., Hung, M. C., Chiocca, S. M., Manning, J., Zhao, X. Y., Fang, K., and Roth, J. A. (1989) *Cancer Res. 49*, 4968−4971.
51. Tackett, A. J., Morris, P. D., Dennis, R., Goodwin, T. E., and Raney, K. D. (2001) *Biochemistry 40*, 543−548.
52. Kopel, V., Pozner, A., Baran, N., and Manor, H. (1996) *Nucleic Acids Res. 24*, 330−335.
53. Brosh, R. M., Jr., Majumdar, A., Desai, S., Hickson, I. D., Bohr, V. A., and Seidman, M. M. (2001) *J. Biol. Chem. 276*, 3024−3030.
54. Kamath-Loeb, A. S., Loeb, L. A., Johansson, E., Burgers, P. M., and Fry, M. (2001) *J. Biol. Chem. 276*, 16439−16446.
55. Peleg, M., Kopel, V., Borowiec, J. A., and Manor, H. (1995) *Nucleic Acids Res. 23*, 1292−1299.
56. Taneja, P., Gu, J., Peng, R., Carrick, R., Uchiumi, F., Ott, R. D., Gustafson, E., Podust, V. N., and Fanning, E. (2002) *J. Biol. Chem. 277*, 40853−40861.
57. Morris, P. D., Tackett, A. J., and Raney, K. D. (2001) *Methods 23*, 149−159.
58. Lebedeva, I., and Stein, C. A. (2001) *Annu. Rev. Pharmacol. Toxicol. 41*, 403−419.
59. Puvvada, M. S., Forrow, S. A., Hartley, J. A., Stephenson, P., Gibson, I., Jenkins, T. C., and Thurston, D. E. (1997) *Biochemistry 36*, 2478−2484.
60. Lukhtanov, E. A., Mills, A. G., Kutyavin, I. V., Gorn, V. V., Reed, M. W., and Meyer, R. B. (1997) *Nucleic Acids Res. 25*, 5077−5084.
61. Hurley, L. H. (1994) *IARC Sci. Publ.* 295−312.
62. Morris, P. D., and Raney, K. D. (1999) *Biochemistry 38*, 5164−5171.
63. Morris, P. D., Byrd, A. K., Tackett, A. J., Cameron, C. E., Tanega, P., Ott, R., Fanning, E., and Raney, K. D. (2002) *Biochemistry 41*, 2372−2378.
64. Maine, I. P., Sun, D., Hurley, L. H., and Kodadek, T. (1992) *Biochemistry 31*, 3968−3975.
65. Scott, G. K., Daniel, J. C., Xiong, X., Maki, R. A., Kabat, D., and Benz, C. C. (1994) *J Biol. Chem. 269*, 19848−19858.
66. Mizuguchi, G., Kanei-Ishii, C., Sawazaki, T., Horikoshi, M., Roeder, R. G., Yamamoto, T., and Ishii, S. (1994) *FEBS Lett. 348*, 80−88.
67. Kumar, R., Shepard, H. M., and Mendelsohn, J. (1991) *Mol. Cell Biol. 11*, 979−986.
68. Sliwkowski, M. X., Lofgren, J. A., Lewis, G. D., Hotaling, T. E., Fendly, B. M., and Fox, J. A. (1999) *Semin. Oncol. 26*, 60−70.
69. Sedelnikova, O. A., Luu, A. N., Karamychev, V. N., Panyutin, I. G., and Neumann, R. D. (2001) *Int. J. Radiat. Oncol. Biol. Phys. 49*, 391−396.
70. Macris, M. A., and Glazer, P. M. (2003) *J. Biol. Chem. 278*, 3357−3362.
71. Sedelnikova, O. A., Panyutin, I. G., Luu, A. N., Reed, M. W., Licht, T., Gottesman, M. M., and Neumann, R. D. (2000) *Antisense Nucleic Acid Drug Dev. 10*, 443−452.
72. Ebbinghaus, S. W., Vigneswaran, N., Mayfield, C. A., Curiel, D. T., and Miller, D. M. (1999) in *Triple Helix Forming Oligonucleotides* (Malvy, C., Harel-Bellan, A., and Pritchard, L. L., Eds.) pp 117−127, Kluwer Academic Publishers, Boston.

BI0273112